

LASER-PULSE MELTING OF NUCLEAR REFRACTORY CERAMICS

C. Ronchi and M. Sheindlin
European Commission
Institute for Transuranium Elements
76125 Karlsruhe, Germany

For
Int. Journ. of Thermophys.

ABSTRACT

An accurate method for melting point measurement of refractory nuclear ceramics was developed, based on laser pulse heating and thermal arrest detection. The temperature measurement is performed by a combined use of a brightness pyrometer and a high-speed spectrometer working in the range 500-900 nm. This method provides both true temperature and spectral emissivity function of the examined materials.

Pure sintered MgO and a Mg:Am mixed oxide were first measured. The resulting melting point of the former ($2350\text{ K}\pm 20$) is significantly higher than that commonly recommended, and decreases by addition of americium.

Furthermore, UO_2 irradiated to 37000 MWd/t and submitted to a reactor loss-of-coolant test was investigated: the melting point decreases from 3120 K, in the as-fabricated state, down to 2950 K. Both fresh Zr:U mixed oxides as well as “corium” lava from a reactor melt-down experiment were finally investigated.

Keywords:

magnesium oxide, zirconium oxide, reactor-irradiated uranium dioxide, americium, corium, melting point, multichannel pyrometry.

1. INTRODUCTION

Under several aspects, the safe performance of nuclear reactors relies on the high melting point of the fuel. In this perspective, not only refractory ceramics consisting of uranium and plutonium compounds are continuously tested, but also inert matrices in which dispersed phases of highly radiotoxic actinides are burnt through nuclear reactions. Moreover, during hypothetical severe accidents where the various core components may interact at high temperatures, ceramic compounds, mostly mixed oxides, represent the principal reaction products. Also in this case the melting point of these reaction products is a crucial parameter on which depends the eventual extent of core meltdown. Therefore, work is still in progress to characterise the melting behaviour of a number of ceramics present in nuclear reactors. Actually, in spite of progress made in high temperature measurements, there is still a great discrepancy in the literature melting data, even for common and widely used materials. This is in part due to the fact that, in conventional furnace melting, perturbations are created by chemical instability of the compounds or reactions with the crucible. On the other side, however, though application of laser heating methods makes it possible to produce melting under very clean conditions, serious disturbances still contribute to produce a loss of accuracy in the melting point determination, i.e.: a) the relatively high vaporisation rate of most ceramic oxides at the melting temperature produces a layer of aerosols that absorbs thermal radiation; b) sample cracking due low thermal shock resistance causes difficulties in controlling the heat exchange of the surface layer with the surrounding, resulting in unstable pyrometric measurements; c) the unknown, mostly variable thermo-optical properties in the vicinity of the melting point make the conversion of brightness to true temperature problematic; d) moreover, since data are demanded for these materials not only in the as-fabricated state, but also after long residence times in reactor, additional handling difficulties are faced due to the high radioactivity of the samples. The method and the experimental set-

up developed in this work, is intended to substantially reduce the above mentioned difficulties and provide accurate measurements of refractory nuclear materials. Two problems are examined in this paper. The first regards use of magnesia as an inert matrix in which dispersed americium is “burnt” by neutrons. The second deals with the melting behaviour of zirconia-urania mixed oxides as reaction products of irradiated uranium dioxide fuel with oxidised zircalloy.

2. EXPERIMENTAL DEVICE

2.1. Heating

The sample is housed in a small cylindrical vessel provided with an optical window, through which both heating and pyrometric measurements are performed. The sample is held by three zirconia pins or mounted in a metallic cylindrical holder of 25 mm diameter; where the space between the holder and the specimen is filled with cement glue. The vessel is equipped with two gas connectors, which enable the internal volume to be rinsed with inert gas. Since some of the examined samples were highly γ -radioactive, a second, *ad-hoc* shielded device was constructed and assembled for the reported melting experiments. In this set-up, the sample vessel is placed in the stainless steel container of a standard lead-shielded transporting device (Fig. 1 shows the scheme of the apparatus). Heating was made by a medium power (350 W) YAG CW-laser. A computer controlled, arbitrary-function generator was used to drive the laser power supply with a time resolution of 1 ms. The laser radiation was transferred to the optical bench of the set-up through a fibre, and was conveyed on the sample surface by a focusing system. This produces a focal spot of 4 to 5 mm in diameter with a very homogeneous power distribution. Self-crucible melting was realised by long (several seconds) controlled laser pulses. The time profile of the pulse was programmed according to the properties of the substance (expected melting temperature, light absorbency, heat conductivity and thermal shock resistance) in order to reach a peak temperature above the

melting point without producing significant axial thermal gradients, and by minimising the risk of crack formation. At the end of the heating ramp, when the conditioning temperature attains a value of $300\text{-}400\text{ K}$ above the melting point, the power is decreased to a stationary level corresponding to approximately $50\text{-}70\%$ of the maximum. Computer code simulation of these melting experiments shows that decreasing the power to this level - instead of completely switching-off the laser – leads, during cool-down, to a significant increase in the duration of the solidification plateau, as well as to a greater temperature stability. In fact, experimental tests confirmed that: 1) undercooling during solidification can be effectively eliminated, and 2) the phase-transition plateau lasts more than $100\text{-}200\text{ ms}$, a relatively long time in this context. In practice, a rather complex power vs. time profile is first programmed and applied to insure smooth heating of the sample up to the maximum temperature. The power is then submitted to a sharp decrease to the lower level, and cooling starts with a surface temperature rate of the order of 10000 K/s . The onset of thermal arrest at the freezing temperature normally results in a pronounced knee in the cooling curve. For compounds of variable stoichiometry, model calculations indicate that at these cooling rates the temperature at the end of the thermal arrest plateau is very near to the solidus (actually, an analysis of the slope of the thermal arrest plateau may furnish information on the liquidus/solidus gap; this analysis is, however, not sufficiently precise at these high cooling rates).

2.2. Pyrometric Method

A monochromatic pyrometer and a fast spectrometer simultaneously perform temperature measurements. The first one is a fast ($10\text{ }\mu\text{s}$ risetime) monochromatic brightness pyrometer ($650\pm 10\text{ nm}$ wavelength, 0.7 mm sighting spot). This pyrometer is working with a Si-detector connected to a very precise log-amplifier and 14-bit precision transient digitiser. The pyrometer was repeatedly calibrated for *brightness* temperature above 2400 K with certified tungsten band lamps. The correction for the presence of the double window of the vessel was

made by spectral absorbency measurements of the window with a standard spectrophotometer. A high-speed spectropyrometer (0.3 mm spot size) is simultaneously used to obtain a proper evaluation of the *true* temperature. This covers the wavelength range of $500\text{-}900\text{ nm}$; the measured spectrum consists of 200 points, which are recorded in circa 4 ms . The buffer of the spectropyrometer enables one to record 32 spectra in 120 ms , with an integration time sufficiently long for the *Si* –array to produce a usable signal. The start of recording is normally synchronised with the onset of the freezing process. The absolute calibration of the spectropyrometer was made against a tungsten-band lamp and a high temperature blackbody model. In this kind of applications, the most important requirement for the spectrometer is good linearity. This was investigated by using a stable light source (tungsten-band lamp) and by varying the integrating time of the diode-array. Since the main source of non-linearity is the current-to-voltage conversion, increasing of the integration time with constant light intensity simulates the increase in light intensity. Actually, the response of all 200 diodes of the array was found to be noticeably non-linear. Since, however, the deviation from non-linearity could be easily compensated with a simple parabolic function, this correction was automatically applied to the primary data. After that, the non-linearity deviations of the photodiode response became negligibly low ($<0.2\%$). An *absolute* intensity calibration at the wavelength of 650 nm was carried out against a tungsten-band lamp. The extension of the calibration to the whole spectral range of $500\text{-}900\text{ nm}$ was made by means of a source of high-temperature blackbody (BB) radiation. This calibration was repeated at several temperatures up to 3200 K . A proof of the adequacy of the BB calibration is that the measured sensitivity curve, defined by:

$$S(T,\lambda)=J_{counts}(T,\lambda)/I_{Plank}(T,\lambda),$$

does *not* depend on the BB temperature. Since the linearity of the system was checked independently, the ratios of the sensitivities taken at different temperatures confirm that, in

the examined wavelength range, the spectral radiance distribution of the BB source does not depend on temperature. It should be noted that any type of direct measurements could not prove the self-consistency of the BB model. Finally, the following hybrid procedure was adopted for the true temperature evaluation: a) The brightness temperature is measured with the high-precision and high-speed monochromatic pyrometer. b) Analysis of the thermal spectrum (an extension of that described in Ref. ¹) is performed to deduce the spectral emissivity function, $\varepsilon = \varepsilon(\lambda)$, and a previous evaluation of the true temperature (with a precision of approximately 0.2 %). c) The final true temperature is calculated from a), by using the emissivity at 650nm obtained in b), with a precision of the order of 0.1%.

3. MELTING POINT MEASUREMENTS

3.1. MgO

The samples were fabricated in our ceramic laboratory in the form of sintered pellets of 6-mm diameter and 8-mm height, from a high purity powder (<400 ppm impurities). The aimed sintered density was rather low (85% of the theoretical density value) to insure better resistance of the pellets to thermal shocks. The pellets are white at room temperature and do not change in colour after repeated melting under inert gas. Heating by laser irradiation is, therefore, difficult, however, as for most semitransparent ceramic oxides, absorbency in the visible and near IR spectral range increases with temperature. A thermogram of a MgO melting test is shown in Fig. 2; in the inset one can see a plot of the solidification plateau with the position of the spectra recorded during the phase transition. The deduced spectral emissivity curves are shown in Fig. 3. In the selected wavelength interval the *effective* emissivity of the liquid is between 0.95 and 1, whilst during solidification it decreases down to 0.92 ± 0.1 . The spectral emissivity at the melting point appears to be effectively constant (only two absorption peaks due to alkali impurities in the vapour are detected), except in the lowest wavelength segment, where a decrease of $\varepsilon(\lambda)$ is observed. The evaluation of the true-

temperature accuracy depends principally on two related experimental conditions: the actual transparency of the sample and the existence of positive thermal gradients between the sample surface and the underlying layer. Experiments were therefore carried out at different cooling rates, producing larger axial gradients. In fact it was observed that the effective emissivity at the freezing point increases with the cooling rate, revealing a contribution of hotter internal layers to the measured spectrum. Yet, by varying the cooling rates below a sufficiently low value, the effective emissivity remains constant. Obviously, this does not excludes bulk contribution effects, however, the correctness of the measurement is corroborated by the coinciding temperature values obtained from the spectral analysis (based on *fractional* spectral intensities) and from the *absolute* signal of the brightness pyrometer. The solidification point was finally determined at $3250 \pm 20 \text{ K}$.

A mixed oxide MgO : 1.5 at. % AmO_2 was then measured. This oxide, also in the form of high density sintered pellets, is dark-grey coloured. Since sintering started from a mechanically blended powder, a preliminary laser pulse was applied, after which americium was homogeneously dissolved in the molten region. This appeared black at visual inspection: actually, a high emissivity was measured ($\epsilon_{600 \text{ nm}} = 0.78$), that corresponds to the *real* spectral emissivity, for the optical transmittance of this mixed oxide is negligible. In Fig. 4 are plotted the thermograms of two pulses with the respective laser power histories: the first one (2), reaching approximately 3100 K , does *not* exhibit any freezing plateau, while the other (1), peaked at 3500 K , shows a clear re-calescence plateau at 3220 K . This temperature corresponds to the solidus point of the sample with a precision of approximately $\pm 15 \text{ K}$. The scatter in the freezing point obtained from measurements of three samples was of the same order of magnitude. The accuracy of the true pyrometric temperature is here better than in the case of the white, translucent MgO . The obtained melting point of MgO ($T_m = 3250 \pm 20 \text{ K}$) is significantly higher than that customarily assumed (3100 K). By considering the melting

production and detection method adopted, as well as the quality of the pyrometers used in this work, an error of 150 K in T_m can certainly be excluded. We must, therefore, conclude that the previous measurements were systematically spurious in defect. Actually, alternative classical melting experiments on MgO produce relevant sources of errors, the major of which is probably caused by the high equilibrium vapour pressure of this oxide (the boiling point is just above the melting temperature) accompanied by chemical dissociation processes. Furthermore, there are only very few measurements published in the literature, and only two – carried out, respectively, in 1913 and 1961 - are considered in the most recent critical review ² as acceptably precise ($\pm 30\text{K}$) ^{3 4}. The melting detection methods used in these experiments are, however, only qualitative (based on sample visual inspection after quenching), and the temperature measurements present unclear aspects. Moreover, melting was produced in crucibles of tungsten, and this element was eventually found in the molten sample with concentrations of the order of 0.1% . Perturbations were, however, also present in more recent melting point measurements ⁵ obtained by laser heating, where a largely understated value of 2870 K was deduced. Some light on this difficulty was cast by the work of Petrov et al., which, in a detailed analysis of the thermal radiation characteristics of MgO and other translucent materials, have shown ^{6 7} that temperature measurements by conventional pyrometers may be heavily spurious, especially if temperature gradients are present. These authors suggested that the melting temperature of MgO might fall between 3215 and 3230 K ⁸. Now, with the pyrometric method developed in this work, the sources of errors exposed by these authors are avoided, and the reported value of the melting point ($T_m=3250\pm20\text{ K}$) is in line with a realistic analysis of the radiative properties of this ceramic.

3.2. $\text{ZrO}_2\text{-UO}_2$

The second case examined is the melting behaviour of the phase produced by chemical interaction of uranium dioxide pellets with their zircalloy cladding at high temperature and

under oxidising conditions. The sample, basically a $(\text{Zr,U})\text{O}_2$ mixed oxide, was obtained from the CEA reactor experiment PHEBUS, where a medium burn-up fuel assembly was submitted to a loss-of-coolant (LOCA) test. No precise melting data were available neither for the irradiated fuel nor for the final reaction product. Moreover, though the ternary phase diagram Zr-U-O was studied since the end of the fifties, experimental data on melting are scanty and date back of more than four decades^{9 10 11 12}. In this work, measurements were then carried out on as fabricated ZrO_2 as well as on $(\text{Zr,U})\text{O}_2$ mixed oxides of selected compositions. The results were then compared to data obtained on irradiated UO_2 and on real *corium* of composition $(\text{U}_{0.6}\text{Zr}_{0.4}\text{X})\text{O}_2$, where X is a set of minor metallic components of less than 5% concentration. The results are reported in Table I and Fig. 5. The measurements on as fabricated materials confirm¹³ that the pseudo-binary phase diagram $\text{UO}_2\text{-ZrO}_2$ exhibits a eutectic at about 2800 K and $\text{U/Zr}=1.1$. At this composition, the measured thermograms *do not* exhibit the effects of a liquidus/solidus temperature gap. The composition of the liquid appears to be the same as that of the f.c.c solid solution. This explains the stability and the excellent reproducibility of the melting point even after repeated shots. The other solidus measurements in mixed oxides with, respectively, 20% and 80% Zr are in agreement with the measurements of Lambertson⁹, showing an almost constant value of the solidus temperature in the range between the eutectic composition and 80% Zr. Also the melting point of pure zirconia (2950 ± 10 K) is within the scatter of the literature values. Particularly interesting are the results obtained on samples of molten corium. These samples were extracted from a large lava mass, produced in the reactor core meltdown experiment PHEBUS-FPT1. The composition of the sample, measured by EDAX, is close to that of the eutectic. The melting experiments were particularly difficult for the sample contained a considerable amount of volatile impurities. In fact, during the first shot, the heat-up flank of the thermogram appears to be strongly perturbed, already at low temperatures (Fig. 5). Actually, the observed random

fluctuations cannot be attributed to a variation of the surface reflectance, but rather to emission of gas and vapours from the surface of the sample. Though the maximum temperature reached during the laser pulse ($T_{peak} > 3500\text{ K}$) ensured formation of a large molten pool, the perturbation of the thermal radiation continued until the laser was switched-off. In the second shot, however, the produced heating stage was much more regular. Only after about 300 ms , at temperatures above 3000 K , did the vapour emission perturbation reappear. A stable thermal arrest in the cooling stage is detectable already in second pulse. A sufficiently precise solidus temperature of $2760 \pm 20\text{ K}$ was measured in the fourth pulse, i.e. about 50 K below the eutectic of the mixed oxide. This difference is likely due to the presence of iron impurities. In fact, a measurement carried out on a second sample containing approximately 10% Fe produced a markedly lower solidus temperature. Finally, the melting point of a pellet of UO_2 irradiated up to 37.000 MWd/t and adjacent to the molten mass of corium was measured. Most of the pellet volume was still intact after the in-pile test, but the cladding and part of the fuel in contact with the molten corium was corroded away. Microprobe analysis shows that the fuel contained, in addition to fission products, approximately $8\text{ to }20\text{ at\%}$ zirconium coming from interaction with the molten cladding. Even in this case, vapour emission did strongly perturb the first pulse, however, in subsequent pulses, gas or aerosol emission was no longer detected, and the cooling stage exhibits regular features (Fig. 6). Analogously to molten corium, the measured melting point of $2950 \pm 20\text{ K}$ is approximately 150 K lower than in the fresh fuel and only slightly lower than the solidus temperature of the mixed oxide with the corresponding Zr concentration.

4. CONCLUSIONS

- Melting of pure and americium-doped magnesia and zirconium-uranium mixed dioxides was produced by direct laser heating under conditions where the molten mass was mechanically stable and homogeneous in temperature. The freezing point was measured on

cooling, at the temperature of the thermal arrest, which remained constant during a few tenths of seconds. Combining spectral and brightness pyrometry enabled temperature to be measured with a fairly good accuracy also in semitransparent materials like MgO and ZrO₂. The measured *effective* spectral emissivity was deduced from the analysis of the thermal emission spectrum in the range 500-900 nm, detected by a 200 spectral windows fast spectrometer, whilst for opaque materials the *real* spectral emissivity was obtained with the same type of analysis.

- The melting point of MgO was measured at 3250 ± 20 K, i.e. approximately 150 K higher than previously reported in the literature. This high value was confirmed by the measured melting point of MgO:AmO₂ (3220 ± 15 K), a dark coloured material, for which pyrometric temperature measurements are much easier.
- The melting point of reactor irradiated UO₂ (37000 MWd/t burn-up) in contact with liquid corium was measured with the same method. A significant decrease of T_m from 3110 K, measured in the as-fabricated fuel, down to 2950 K was observed. The decrease in T_m , which remains unchanged even after repeated pulses, is due to the effect of intake of zirconium and to fission products soluble in solid UO₂.
- The three measured solidus temperatures of uranium-zirconium mixed oxides falls 10-20 K below the solidus line previously measured by Lambertson. One measurement of a molten corium sample at 37000 MWd/t burn-up, with composition near the eutectic point of the ZrO₂-UO₂ pseudo binary phase diagram, exhibits a melting temperature of only 50 K below the eutectic.

ACKNOWLEDGMENTS

The authors are indebted to the PHEBUS Project and to CEA, Cadarache for permitting publication of data of irradiated materials, to D. Bottomley, for preparing the irradiated samples in his hot cells, and C. Morello for his valuable help in the experiments.

TABLE I
Measured melting point
and corresponding normal spectral emissivity at 650 nm wavelength

<i>Material</i>	<i>Type</i> [*]	<i>T_m (K)</i>	<i>ε(650nm, T_m)</i>
MgO	tt	3250±20	0.92±0.01 ^{\$}
MgO:0.015AmO ₂	d	3220±10	0.78±0.01
UO _{2.00}	d	3110±5	0.86±0.01
ZrO _{2.00}	t	2950±10	0.85±0.01
(U _{0.5} Zr _{0.5})O _{2.00}	d	2805±5	0.85±0.01
(U _{0.8} Zr _{0.2})O _{2.00}	d	2926±3	0.86±0.005
(U _{0.2} Zr _{0.8})O _{2.00}	d	2810±5	0.89±0.01
UO _{2.00} :5-7 at% Zr (after a LOCA at 37000 MWd/t)	d/irr	2950±20	0.78±0.02
(U _{0.50} Zr _{0.47} Fe _{0.02} Y _{0.01})O ₂ (after a LOCA at 37000 MWd/t)	d/irr	2760±25	0.88±0.03

- *) tt: *translucid at room temperature and, possibly, at the melting point*;
t: *translucid at room temperature and opaque at very high temperatures*;
d: *dark coloured* ;
irr: *reactor-irradiated sample*
- \$) *effective emissivity*

CAPTIONS OF THE FIGURES

1. Scheme of the set-up
2. Laser-power profile and thermogram showing thermal arrest during MgO freezing.
3. Effective spectral emissivity of MgO during freezing and just above the melting point.
The sharp absorption wells are due to alkali impurities in the surrounding atmosphere.
4. Effect of two consequent pulses applied to americium-doped magnesia. Whilst pulse (1) produces a clear thermal arrest at 3220 K, that labelled (2), with a maximum temperature just below 3000 K, does not produce melting.
5. Thermograms of successive pulses on irradiated corium, basically consisting of a uranium-zirconium mixed oxide. The first pulses are strongly perturbed by release of volatile fission products and adsorbed gases.
6. Thermogram of pulse melted UO_2 rated at 37000 MWd/t in a Light-Water Reactor.
The material interacted with molten zircalloy and contained 5 to 7 % Zr.
7. Measured solidus of $\text{UO}_2\text{-ZrO}_2$ mixed oxides. The full diamonds corresponds to measurements on pure samples. The arrows indicate reactor-irradiated samples. The full lines correspond to the data of Lambertson.

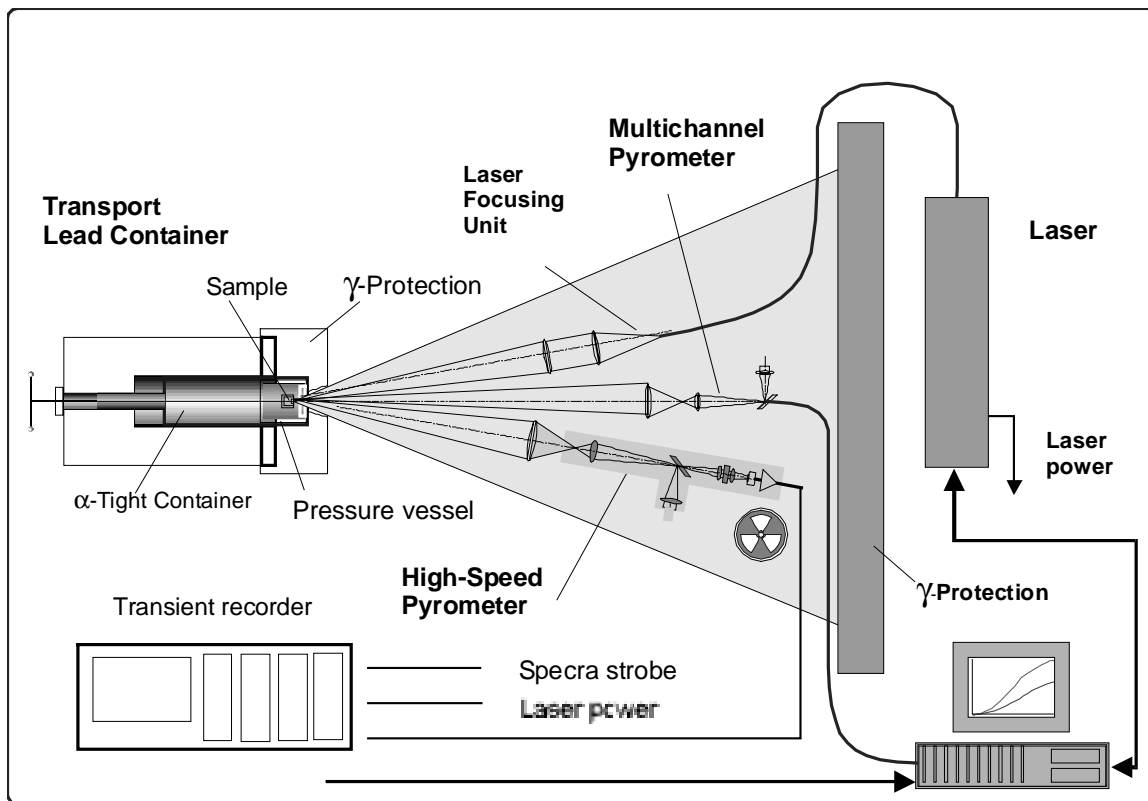


Fig. 1

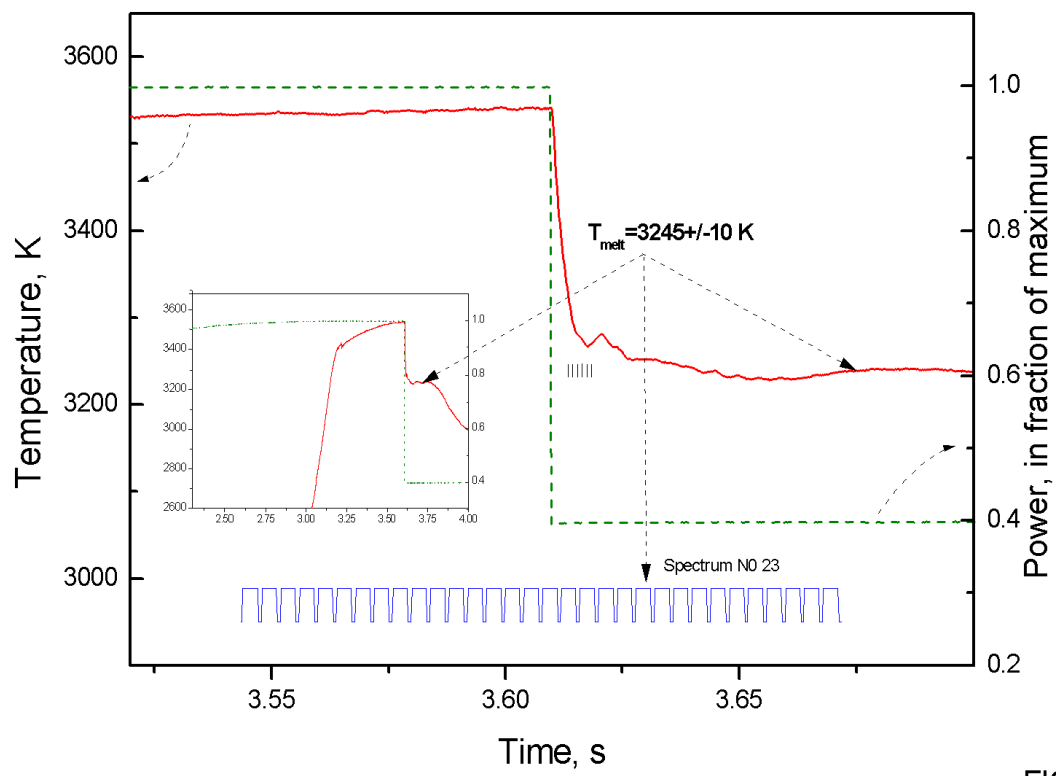


FIG. 2

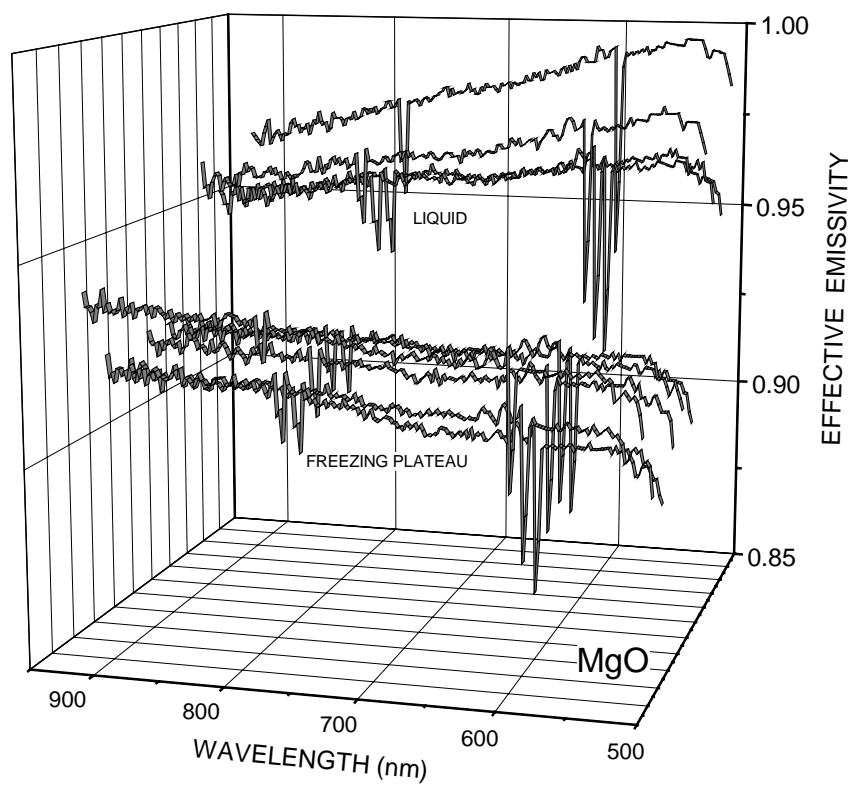


FIG.3

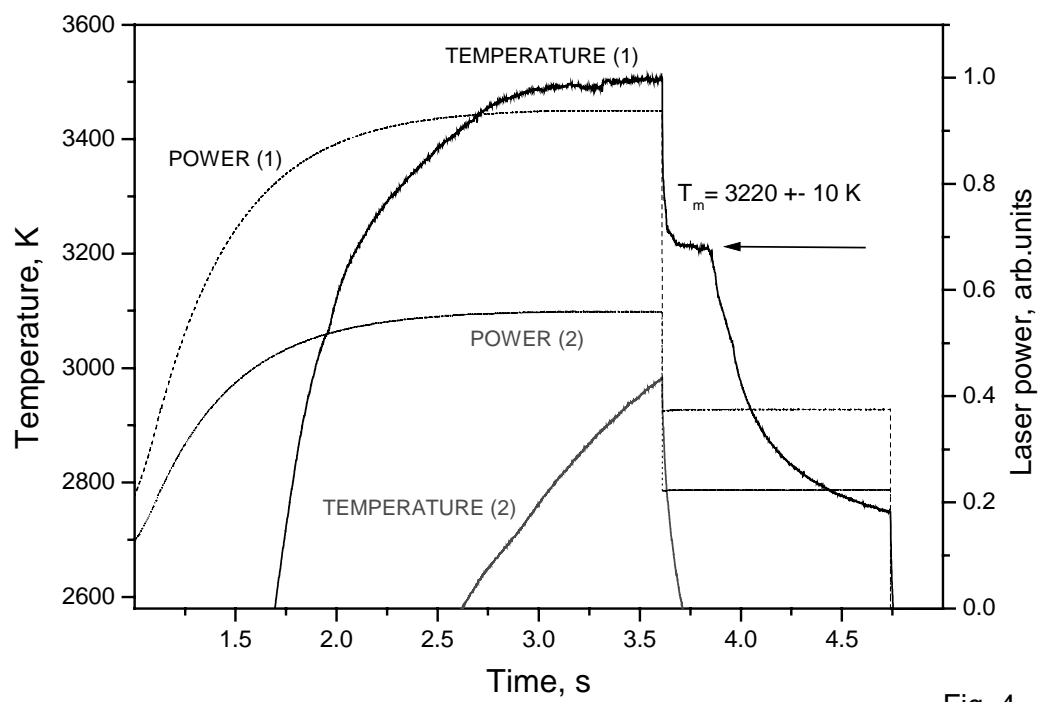


Fig. 4

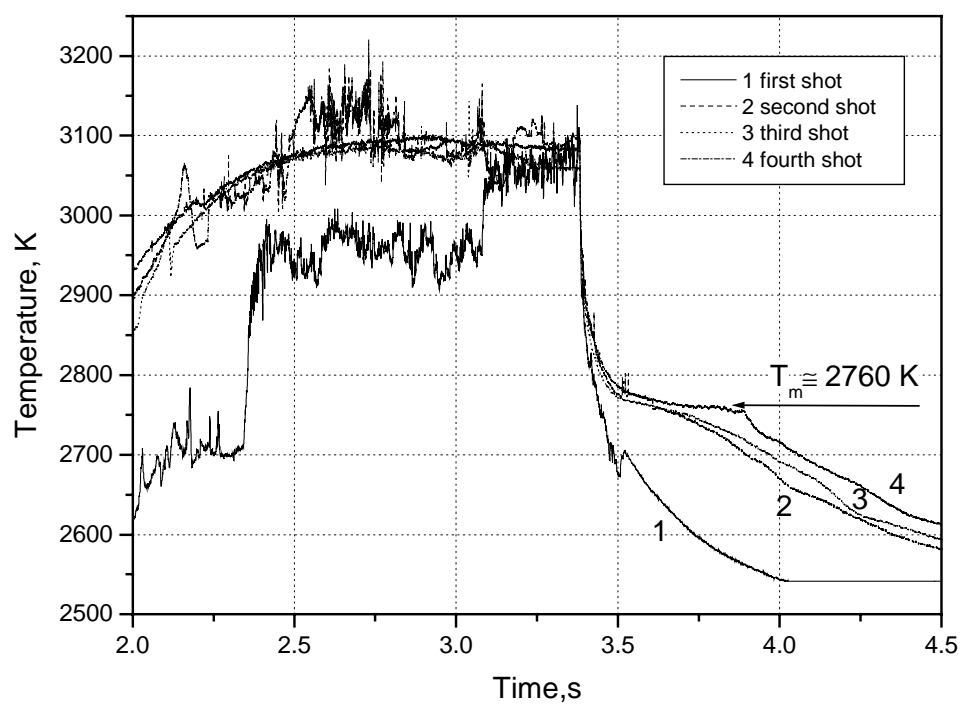


Fig.5

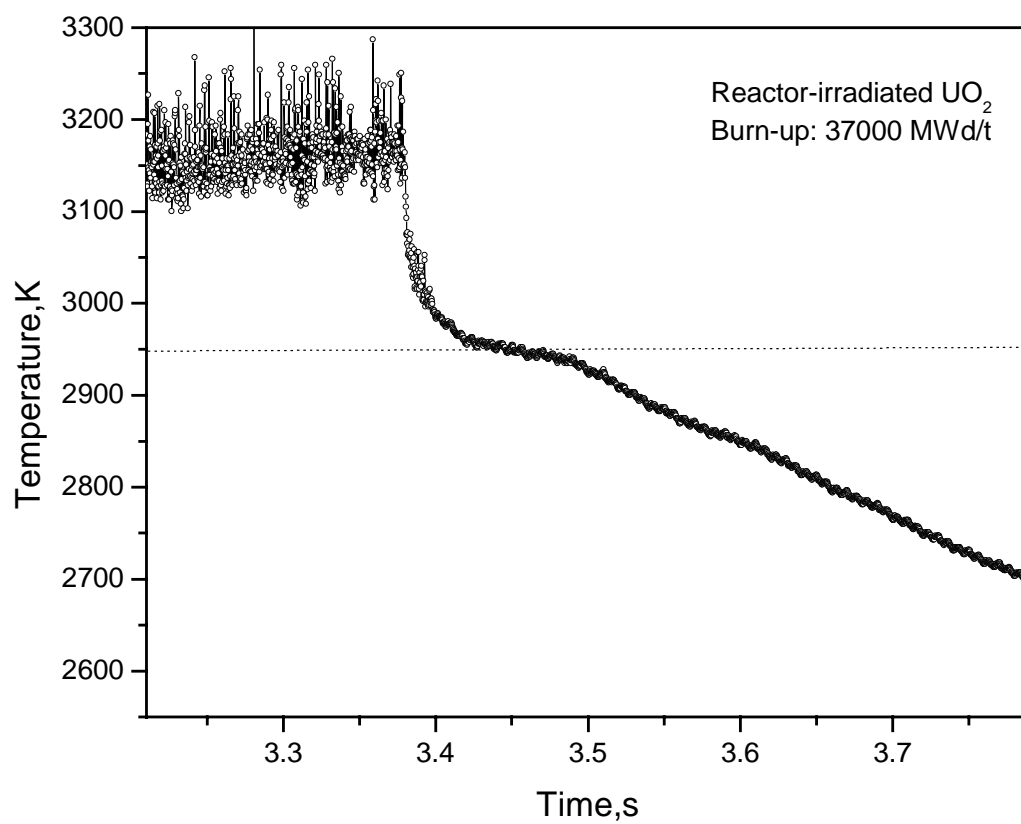


Fig. 6

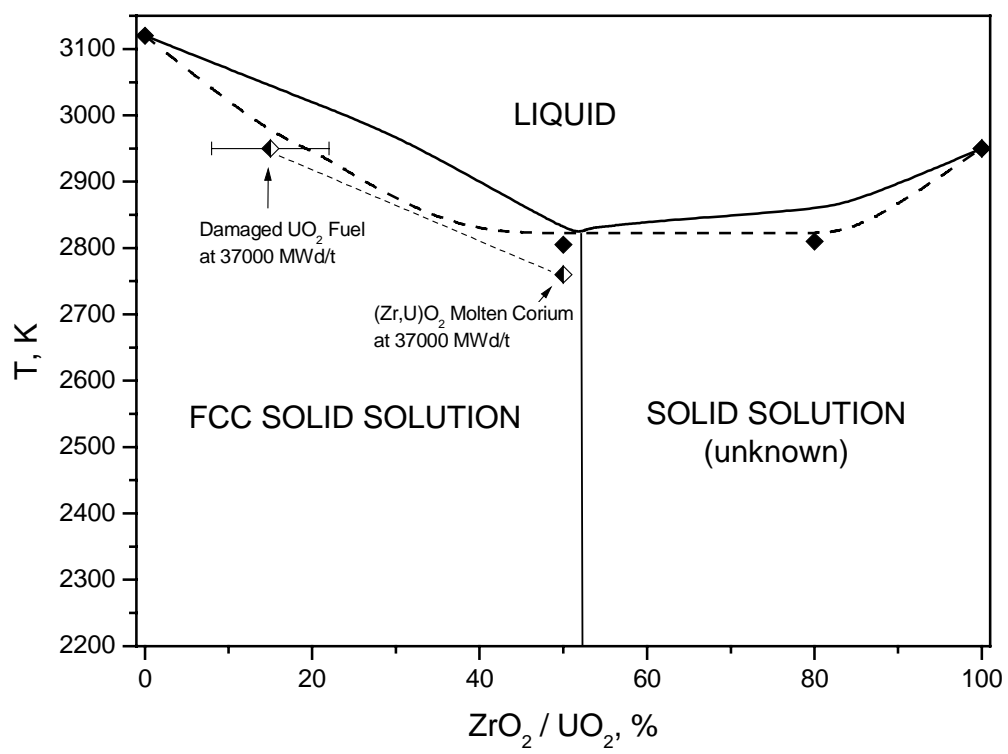


Fig. 7

REFERENCES

-
- ¹ C. Ronchi, J. P. Hiernaut and G. J. Hyland, *Metrologia* **29**: 261(1992)
- ² L. V. Gurvich et. al. "Thermodynamic Properties of Individual Substances", Vol. 3, (Begell House CRC Publ. London ,1994), p.397
- ³ C. W. Kanolt, J. Wash. *Acad. Sci.* **3**: 315 (1913)
- ⁴ R. N. McNelly, F. I. Peters, P. H. Ribbe, *J. Amer. Cer. Soc.* **44**, 10: 491 (1961)
- ⁵ M. Bober, H. U. Karow and K. Mueller, *High Temp.-High Press.* **12**, 2: 161 (1980)
- ⁶ A. Yu. Vorobev, V. A. Petrov, V. E. Titov and A. P. Chernyshev, *Tepl. Vys. Temp.* **30**, 2:181 (1992)
- ⁷ A. Yu. Vorobev, V. A. Petrov, V. E. Titov and A. P. Chernyshev, *High Temp.-High Press.* **31**: 227 (1999)
- ⁸ G. E. Valyano, A. Yu. Vorobev, V. A. Petrov, V. E. Titov and A. P. Chernyshev, *Tepl. Vys. Temp.* **30**, 5: 923 (1992)
- ⁹ W. A. Lambertson, M.H.Mueller, *J. Amer. Ceram. Soc.* **36** :365 (1953)
- ¹⁰ G. M.Wolten, *J. Amer. Ceram. Soc.* **80**: 4772 (1958)
- ¹¹ N. V.Voronov et al., Proc. 2nd Conf. on Peaceful Uses of Atomic Energy, 6 (Geneva, 1958) p.221
- ¹² I. Cohen, B. E.Shaner, *Journ of Nucl. Meter.* **9**:18 (1963)
- ¹³ K. A. Romberger et al. *Journ. Inorg. Nucl. Chem.* **29**:1619 (1967)